Proceedings of CHT-15
ICHMT International Symposium on Advances in Computational Heat Transfer

May 25-29, 2015, Rutgers University, Piscataway, USA

CHT-15-221

The numerical modelling of the convection of a Bingham fluid in a porous medium

D. A. S. Rees
Department of Mechanical Engineering, University of Bath,
Claverton Down, Bath BA2 7AY, United Kingdom.
Email: D.A.S.Rees@bath.ac.uk

ABSTRACT We consider the free convection of a Bingham fluid which is saturating a porous medium. Attention is focused on the classical problem of a sidewall-heated cavity. For a Newtonian fluid convection arises at all values of the Darcy-Rayleigh number, but for a Bingham fluid buoyancy forces need to be sufficiently strong to overcome the microscopic yield stress. We consider both an isotropic and an anisotropic form of the Darcy-Bingham law, and numerical simulations are aided by the use of a regularized form of that law. F.A.S. multigrid with line relaxation is used to obtain the streamfunction. We find that stagnation arises in the corners and at the centre of the cavity. As the strength of the yield criterion, as measured by the Rees-Bingham number, increases, convection becomes increasingly confined to the outer regions until full stagnation eventually occurs.

GOVERNING EQUATIONS

The flow of Bingham fluids in porous media is a well-established topic with a variety of important industrial applications particularly some in the oil industry. A Bingham fluid is characterized by having a yield stress by which is meant that the fluid exhibits no rate of strain (equivalently no velocity gradient) unless the local stresses exceed a critical value called the yield stress. In practice this means that the fluid is either stagnant or else moving as a plug. Above the yield threshold the fluid is Newtonian.

In the context of porous media the equivalent statement relates the Darcy velocity to the magnitude of the applied pressure gradient. Therefore the fluid is stagnant when the applied pressure gradient (or, more generally, body forces, which might include buoyancy) is too small. The simplest unidirectional Darcy-Bingham law is given by Pascal [1981],

$$w = \begin{cases} -\Big[1 - \dfrac{\mathrm{Rb}}{|p_z|}\Big] p_z & \text{when } |p_z| > \mathrm{Rb}, \\ 0 & \text{otherwise}, \end{cases} \tag{1}$$

and when buoyancy forces (subject to the Boussinesq approximation) are present this becomes,

$$w = \begin{cases} -\Big[1 - \dfrac{\mathrm{Rb}}{|p_z - \mathrm{Ra}\,\theta|}\Big] \big(p_z - \mathrm{Ra}\,\theta\big) & \text{when } |p_z - \mathrm{Ra}\,\theta| > \mathrm{Rb}, \\ 0 & \text{otherwise}, \end{cases} \tag{2}$$

where the Newtonian forms correspond to $\mathrm{Rb} = 0$. In these equations,

$$\mathrm{Ra} = \frac{\rho g \beta \Delta T K L}{\mu \alpha}, \qquad \text{and} \qquad \mathrm{Rb} = \frac{GKL}{\mu \alpha}, \tag{3}$$

are the Darcy-Rayleigh and Rees-Bingham numbers, respectively. In (3) most of the terms correspond to their usual definitions, but specifically α is the thermal diffusivity, K the permeability, L the height of the cavity and G the yield pressure gradient.

In practice, the location of the yield surface has to be part of the numerical solution, but it is possible to employ a regularization similar to that of Papanastasiou [1987] to soften the effect of the yield threshold by allowing the fluid to have an artifically high viscosity when the pressure gradient is small. Thus Eq. (1) may be replaced by,

$$w + \mathrm{Rb}\tanh cw = -p_z, \tag{4}$$

where c is an adjustable parameter. The threshold model is obtained as $c \to \infty$.

There are now two main ways of extending these equations for two-dimensional flow. The first is to insist that the medium is isotropic and hence we require frame invariance. The second is to assume that the porous medium consists of a square grid of narrow channels. For the isotropic case the Darcy-Bingham law for two dimensional convection is,

$$\Big[1 + \mathrm{Rb}\,\frac{\tanh(cq)}{q}\Big]u = -p_x, \quad \Big[1 + \mathrm{Rb}\,\frac{\tanh(cq)}{q}\Big]w = -p_z + \mathrm{Ra}\,\theta, \quad \text{where} \quad q^2 = u^2 + w^2, \tag{5}$$

while the square-network anisotropic version is,

$$u + \mathrm{Rb}\,\tanh(cu) = -p_x, \qquad w + \mathrm{Rb}\,\tanh(cw) = -p_z + \mathrm{Ra}\,\theta. \tag{6}$$

When the streamfunction is introduced according to $u = -\psi_z$ and $w = \psi_x$, these models become,

$$\nabla^2\psi + \frac{\mathrm{Rb}\,\tanh(cq)}{q^3}\Big[\psi_z^2\psi_{xx} - 2\psi_x\psi_z\psi_{xz} + \psi_x^2\psi_{zz}\Big] + \frac{\mathrm{Rb}\,c\,\mathrm{sech}^2(cq)}{q^2}\Big[\psi_x^2\psi_{xx} + 2\psi_x\psi_z\psi_{xz} + \psi_z^2\psi_{zz}\Big] = \mathrm{Ra}\,\theta_x, \tag{7}$$

where $q^2 = \psi_x^2 + \psi_y^2$, and

$$\Big(1 + \mathrm{Rb}\,c\,\mathrm{sech}^2(c\psi_x)\Big)\psi_{xx} + \Big(1 + \mathrm{Rb}\,c\,\mathrm{sech}^2(c\psi_z)\Big)\psi_{zz} = \mathrm{Ra}\,\theta_x. \tag{8}$$

In both cases the heat transport equation is given by,

$$\theta_t = \nabla^2\theta + \psi_z\theta_x - \psi_x\theta_z. \tag{9}$$

We confine attention to a square cavity. The boundary conditions are that $\psi = 0$ on all four boundaries. We set $\theta = 1$ at $x = 0$ and $\theta = 0$ at $x = 1$ while the surfaces at $y = 0$ and $y = 1$ are insulated.

These equations were solved using a finite difference discretisation on a 65×65 grid. Steady state solutions were obtained by adopting a Full Approximation Scheme multigrid method with V-cycling and pointwise relaxation. Convergence to the steady state was deemed to have taken place once the residual for the heat transport equation was less than 10^{-10}. The largest numerical error arises when Ra = 100 and Rb = 0; the numerical solutions are then within 0.3% of the exact solution.

NUMERICAL SOLUTIONS

A selection of streamlines and isotherms for Ra = 100 are presented in Fig. 1 for the isotropic model which shows the effect of having different values of Rb. The Rb = 0 case corresponds to Newtonian flow and when Ra = 100 there is a significant deformation of the isotherms from being vertical, the pure conduction state. When Rb grows from zero one sees a region of stagnation appear in the centre of the cavity where the flow is at its weakest. The stagnant region grows as Rb increases given that buoyancy

is rendered less effective as the yield pressure gradient increases. Eventually, when Ra = 20, convection arises only within a narrow circuit around all four surfaces. The numerical evidence, together with a network analysis in Rees [2015], suggests that flow is extinguished once Rb reaches 25. More generally flow arises once Ra > 4Rb. Thus when Rb = 25 in Fig. 1 the presence of the streamlines in what is supposed to be the stagnant region is an artifact of the regularization: although more of the flow takes place in the unshaded region its weakness is shown by the near-verticality of the isotherms.

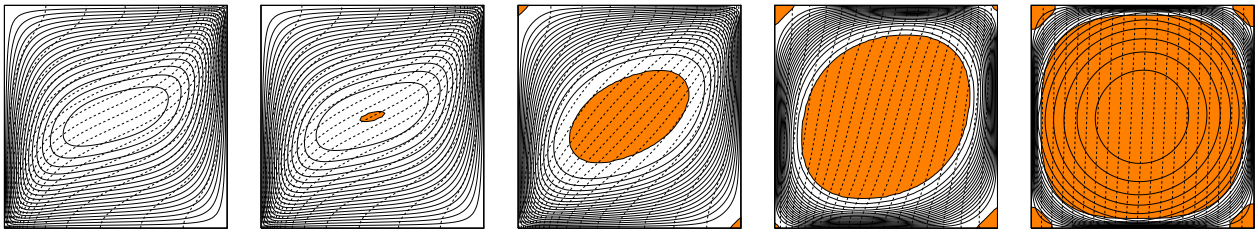

Figure 1. Streamlines (continuous) and isotherms (dashed) for $c = 10$ and Ra = 100 using the isotropic model. The stagnant regions are shaded in orange.

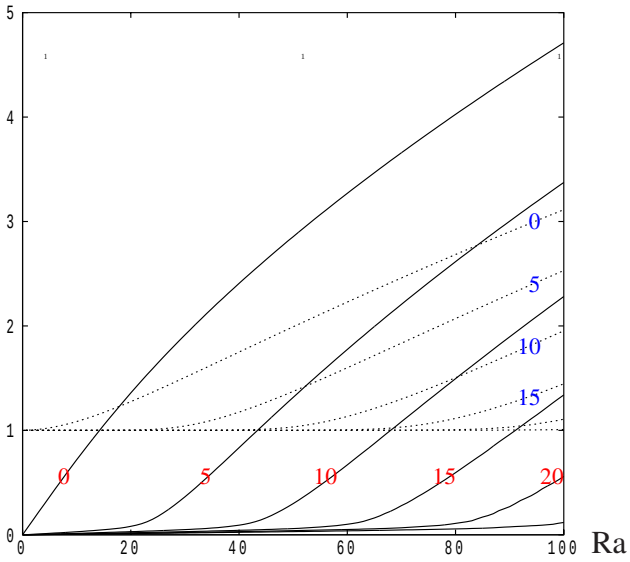

Figure 2. Variation of $|\psi|_{\max}$ (continuous) and Nu (dashed) with Ra for Rb = 0, 5, 10, 15, 20 and 25.

Figure 3 shows the change in streamline and isotherm patterns when the anisotropic model is adopted for the case Ra = 100. The regions shaded in red (yellow) denote cases where fluid is constrained to flow horizontally (vertically) because the effective vertical body force is insufficient to overcome yield in the vertical (horizontal) microchannels. For this type of microstructure the shape of the fully stagnant region is quite different from that of the isotropic model. When Rb = 20, the resulting flow is almost entirely either purely horizontal or purely vertical. The fully stagnant region is almost exactly square, and there are small turning regions in the corners where, for example, a vertical boundary layer empties into a horizontal one. Once more we see a reduction in the isotherm deformation as Rb increases, and the flow ceases once Ra exceeds 4Rb [Rees 2015]. The variation of the flow strength and the mean rate of heat transfer behave in the same way as in Fig. 2 and are omitted for brevity.

Figure 4 represents a similar microstructure except that the channels are orientated at ±45° to the coordinate directions. The governing momentum equation which replaces Eqs. (5) and Eq. (6) is much

longer and is therefore omitted here, again for the sake of brevity. Given what was seen in Fig. 3, the pattern and evolution of the regions of partial and full stagnation are as one might expect. When Rb = 20 the 'racetrack' pattern of streamlines, which lay close to the walls for Rb = 20 in Figs. 1 and 3, now occupies an almost square region aligned at 45° to the cavity boundaries. This case represents one where Rb is just below the value for which full stagnation occurs. A network model approach will be required to be able to find the relationship between Ra and Rb for this microstructure.

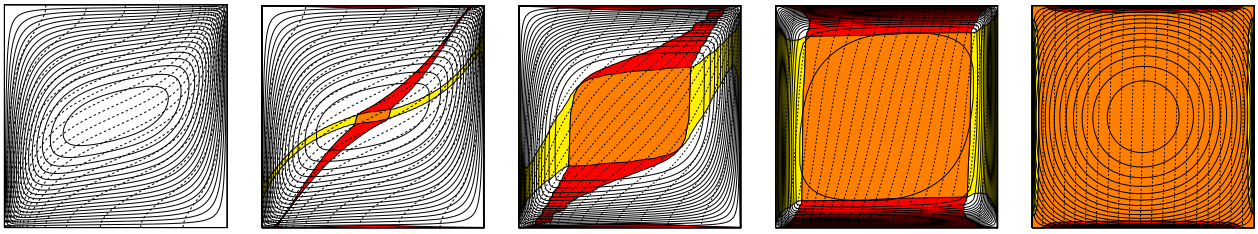

Figure 3. Streamlines (continuous) and isotherms (dashed) for $c = 10$ and Ra = 100 using the isotropic model. The red and yellow regions depict 'stagnation' in the vertical and horizontal directions, respectively. Orange again represents full stagnation.

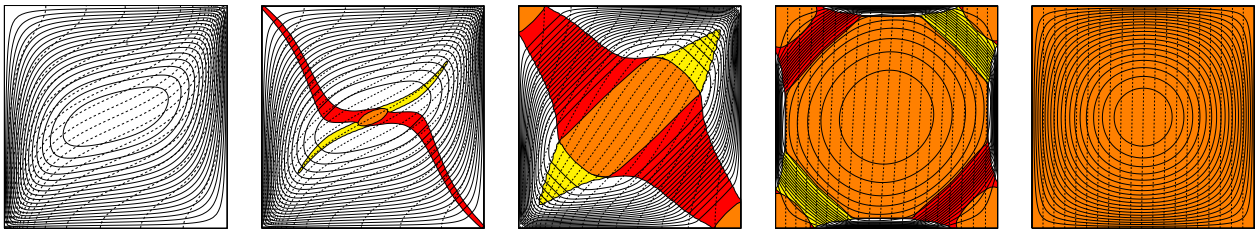

Figure 4. Streamlines (continuous) and isotherms (dashed) for $c = 10$ and Ra = 100 using the isotropic model. The red and yellow regions depict 'stagnation' in one direction or the other of the underlying microchannels.

CONCLUSIONS

When a sidewall-heated porous cavity is saturated by a Newtonian fluid then free convection arises at all values of the Darcy-Rayleigh number. In this paper we have seen that, when a Bingham fluid saturates the medium, then convection arises only when Ra exceeds 4Rb for the isotropic medium and the first anisotropic model which confirms the network modelling of Rees [2015]. The critical value of Ra is larger for the second anisotropic model because the direction of buoyancy is misaligned with that of the microchannels. We have also found that a regularization of the standard threshold model of the Darcy-Bingham law allows for a straightforward use of standard iterative methods to solve the resulting nonlinear Poisson's equations for the streamfunction.

REFERENCES

Papanastasiou, T.C. [1987], Flow of materials with yield, *Journal of Rheology*, Vol. 31, pp. 385–404.

Pascal, H. [1981], Nonsteady flow through porous media in the presence of a threshold gradient, *Acta Mechanica*, Vol. 39, pp. 207–224.

Rees, D.A.S. [2015], Convection of a Bingham Fluid in Porous Media, *Handbook of Porous Media III* ed. K.Vafai. (Taylor and Francis). To appear as Chapter 17.